

Parameter Impacts of Martensitic Structure on Tensile Strength and Hardness of TIG Welded SS410 with characterized SEM Consequences

G. MAHESH, D. VALAVAN, N. BASKAR, A. BOVAS HERBERT BEJAXHIN*

Abstract: Consuming various TIG welding settings, the impact of mechanical properties on the butt joint of 410-Martensitic Stainless Steel Plate is explored. Mechanical properties such as tensile strength and hardness are evaluated on the welded butt junction plates using three levels of 200 A, 220 A and 240 A welding currents and the electrode diameters of 1.5, 2 and 2.5 mm and four factor parameters of inputs. Welding current, wire feed rate, electrode diameter, and gas flow rate are set as input parameters. The optimal input responses of welding current, electrode diameter, wire feed rate, and gas flow rate are employed over the 27 sample specimens based on array L27 Design of Experiment tool. The input parameters 240 A of welding current have improved significantly over the structural changes on martensitic form which is evidenced by their multiple SEM Micrographs, as it can be seen in the Hardness up to maximum of 512 BHN and the Tensile strength of 1090 N/mm² outcomes.

Keywords: hardness; martensitic steel; novel SEM microstructures; tensile test; tungsten inert gas welding

1 INTRODUCTION

Martensitic stainless steel is employed in the fabrication industry despite its remarkable corrosion resistance and ability to withstand high temperatures. Crane pins, gears, valve stems, satellite components, actuators, hydraulic rams, conveyor drive systems, mixing blades, and petrochemical industries are just a few of the applications for 410-martensitic stainless steel. Due to its raised high corrosion resistance and thermal toughness, type 410 Martensitic stainless steel is primarily employed in fabrication industries among the 300 series grade stainless steels. One of the finest fusion welding processes for the fabrication sectors is Tungsten Inert Gas (TIG). Tungsten Inert Gas (TIG) welding is relatively new technique of electric arc metal joint welding process without applying pressure for Aluminum, Mild Steel, and various graded Stainless steel and arc is formed between a nonstop Cu coated wire and work plate. The TIG welding is selected for 410 martensitic stainless steel butt joints are hardenable and it exposes good toughness characteristics. TIG welding process is not necessary to prepare for pre welding and post welding. TIG welding method is mostly used for automotive parts and steel structural joints. It is a non-consumable electrode used for this welding process and producing heat on the surface of work piece. The 410 martensitic stainless steel is very economical and of good correction resistance for petrochemical, pressure vessel, valves, food industries, tanks and pumps. Most researchers have explored various grades of stainless steel using TIG welding, Gas Metal Arc Welding (GMAW), and Metal Inert Gas Welding (MIG) with various input and output response analyses.

[1] Neeraj Sharma et al. (2020) analysed the input factors (shielding gas, electrode diameter, gas flow rate, groove angle and welding current) that affect the output responses, i.e., tensile strength and hardness of the SS202 weld metal. The results show that the 1.5 mm diameter electrode has the highest tensile strength. The factors such as 15 l/min of gas flow rate, 240 A of welding and a 60° groove angle were used. The most significant factor, with a *P* value of 0.009, was found to be welding current, which caused a difference in hardness at the weld field. With the welding current from 160 to 240 A, the hardness of the weld area appears to decrease significantly. By using

Taguchi techniques to improve welding parameters and fractures, [2] Rizvi and Ali (2018) were able to improve various welding parameters that affect the weldability of SS304H. The orthogonal array L9 is employed. To control the effect of various welding parameters like gas flow rate, wire feed speed, and welding current on the weldability of Stainless Steel 304H, statistical techniques such as analysis of variance (ANOVA), signal to noise ratio (SNR), and other statistical techniques are used. [3] Loureiro and Rodrigues. (2008) aimed to develop activating fluxes to improve weld bead geometry and increase weld penetration depth in austenitic stainless steels. Titanium and Aluminium oxides are the two homemade fluxes that have effects on the bead geometry. The mixture of Argon and argon/helium gases was used for this investigation. A significant value of penetration was achieved for the best parameter of welding currents for argon and helium shielding gases. It is clearly observed that the welding current is a vital role for this experiment.

[4] Ahmadi and Ebrahimi (2015) analysed the mechanical properties of 316 austenitic stainless steel. Investigation outputs specified the maximum depth/width ratio of stainless steel for various oxides with different coating levels. [5] Vasudevan (2017) analyzed the minimum value of 50 ppm of sulphur that is attained for the best penetration of the weld in 316LN stainless steel. The grade of 316LN and 304LN stainless steel made good weld property with minimum usage of base metal. [6] Himanshu Garg et al. (2019) have reported reviews on the TIG and A-TIG welding processes of Austenite Stainless Steel (ASS) which include numerous recent experimental work and also good mechanical properties. [7] Ghosh et al. (2016) experiments were conducted to investigate the effect of nozzle, current, and gas flow rate to plate distance on weld eminence in metal gas arc welding of Austenitic stainless steel AISI 316L. The results calculated are in the form of influence from each parameter, through which best parameters are recognized for the highest tensile strength and good percentage of elongation. [8] G. Mahesh et al. (2017) have investigated the mechanical behaviour of aluminum material by using Design of Experiment (DOE) L9 orthogonal array in sand casting process. [9] Maheshwaran, and Senthilkumar (2017) have analysed the mechanical properties of stainless steel using MIG welding. Different mechanical tests including hardness and

tensile are carried out to identify the microstructure of the welded specimens [10]. Somani and Lalwani (2019) have used the Design Expert software to mathematically evaluate and optimise control parameters. Significant control factors are used to create a numerical model [11]. Singhmar and Verma (2015) investigated the effects of welding parameters on the mechanical properties of grade 304 austenitic stainless steel (AISI 304) using Gas Metal Arc Welding (GMAW) at various welding parameters. [12] Feng et. al. (2015) discussed the corrosion behavior of stainless steel grade AISI 316L using TIG welding. The authors of this study examined and verified minimum thickness of 10mm welded with single pass.

[13] Bharwal and Vyas (2014) discussed the welding characteristics of SS202 with Gas Tungsten Arc Welding and it is associated with the butt joint of SS304. It is used for various applications in automotive industry and also indoor applications. The mechanical properties of two dissimilar welded joints of stainless steel (SS316 and S S202) alloys were optimised by [14] Rekha and Kajal (2018). An L9 Orthogonal Array was used to schedule the experiments, and the hardness and toughness were used as output parameters for this investigation. The experiment was based on predicted mechanical characterization of SS AISI 316 & 304 using TIG & MIG welding processes, according to [15] Suresh Kumar et al. (2011). The metal properties like grain structure, ductility, hardness, strength, and HAZ were inspected in both tungsten inert gas and metal inert gas welding with constant voltage. Using friction stir welding, [16] Amir Ghiasvand et al. (2020) studied the different temperature distributions with different offset techniques for AA6061 and AA5086 alloys. In this inquiry, optimization techniques were employed to determine the maximum temperature for each experiment. [17] Kazemi and Ghiasvand (2021) examined friction stir welding on AA6061-T6 aluminium alloys in both its symmetrical and asymmetrical forms. Lower and upper surfaces of the workpiece are used for friction welding. Tensile specimens are prepared for the experiment work samples, and their mechanical characteristics are examined. Surface quality can be assessed on heat-treated and non heat-treated specimens using machining parameters and simulations. The optimised result helps locate the ideal surface roughness solution. The grain sizes of various welded portions made of the alloy AA6061-T6 were examined by [18] Ghiasvand et al. (2020). The wear and tribological properties can be easily carried out with the optimization and simulations by [19] Bejaxhin et al. (2021). In this inquiry, friction stir welding is performed, and finite element simulation is used to investigate the various friction stir welding parameters.

Based on the literature review, the various TIG welding parameters are analysed and optimized the best

parameters recommended to the fabrication industries. TIG welding parameters are used to analyse various weld materials such as SS302, AISI 304, AA6061, AISI 316L, SS202, and SS316 for various welding joints. The 410 martensitic stainless steel is used as the work piece for the butt joint in TIG welding with various welding parameters in this study. In the following section, the experimental methods and tensile test specimen are also discussed.

2 MATERIALS AND METHODS

Compositions of weld material and filler rod are clearly explained in this research work. The details of welding current, electrode diameter, wire feed rate and gas flow rate are selected according to the standard of TIG welding machine

2.1 Weld Material

In this investigation, the 410 martensitic stainless steel is selected as a work piece material. The dimensions of the AISI 410 plate for TIG butt welding such as length, breadth and thickness are 130, 60 and 5mm respectively. The experimental work is carried out on TIG welding machine (Everlast Power kit, TIG 400 A) and it is available in Saranathan College of Engineering, Tiruchirappalli, Tamil Nadu 620014, India, as shown in Fig. 1.



Figure 1 TIG welding Machine (Everlast Power kit, TIG 400 A)

The equality ratio of the chemical composition of SS308 is mostly present in 410 martensitic stainless steel. So it is very suitable to act as a filler rod for these experiments. The chemical composition of filler rod and base plate for this welding process is as given in Tab. 1. The contribution of Silicon (Si), Chromium (Cr) and Nickel (Ni) shows the withstanding of initial strength and its corrosion resistance after the welding. Probably the rust formation also can be avoided by these methods.

Table 1 Chemical composition of base plate and filler rod

Material	%Si	%Cu	%S	%Mn	%C	%Cr	%P	%Ni	Fe
Filler rod	0.3-0.6	0.61	0.02	1.2-2.6	0.05	19.52	0.033	8.91	balance
Base late	0.41	0.01	0.004	2.1	0.05	19.22	0.022	9.1	balance

Design of Experiment (DoE) by Taguchi is one of the most excellent analytical software and it reduced the number of iterations for reaching the best level. In this investigation, four factors like welding current, electrode diameter, wire feed rate and gas flow rate are selected as input welding parameters.

Table 2 Variables and their factors of TIG welding process

Variable	Level 1	Level 2	Level 3
Welding current / A	200	220	240
Electrode diameter / mm	1.5	2.0	2.5
Wire feed rate (IPM)	250	300	350
Gas flow rate / l/min	15	20	25

The output responses like hardness test and tensile test results are selected and the fracture analysis also investigated. The input factors and their levels are given in the Tab. 2.

3 EXPERIMENTAL PROCEDURE

Based on the Design of Experiment, the L27 orthogonal array is selected and the 27 test specimens prepared for this investigation. Tensile test specimens are selected as per ASTM D412 (Type A) standard and shown in Fig. 2. Butt joint welding is performed on 410 martensitic stainless steel using specific TIG welding parameters. Welded test specimens conducted the longitudinal tensile test by using UTM 50T machine.

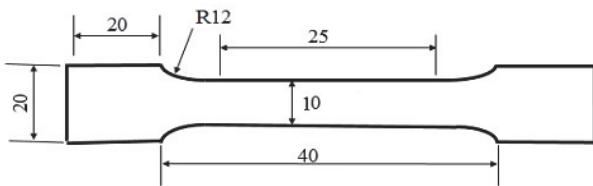


Figure 2 Tensile test specimen as per ASTM D412 (Type A)

Historical data of Experimental Design is used for calculating the number of experimental runs. TIG welding parameters are chosen based on four factors and three levels. Standard parameters are used for all the specimens. Fig. 3 shows the results of twenty-seven butt joint welding experiments using various welding parameters from the TIG welding process.

TIG welded specimens were tested for tensile strength in the UTM Krystal Equipment with range of 40T, ram stroke 0-700 mm and it is shown in Fig. 4. Hardness is measured at three different positions on welded zone using Brinell hardness machine and average values of BHN are

selected in all specimens. The Brinell hardness machine is shown in Fig. 5.

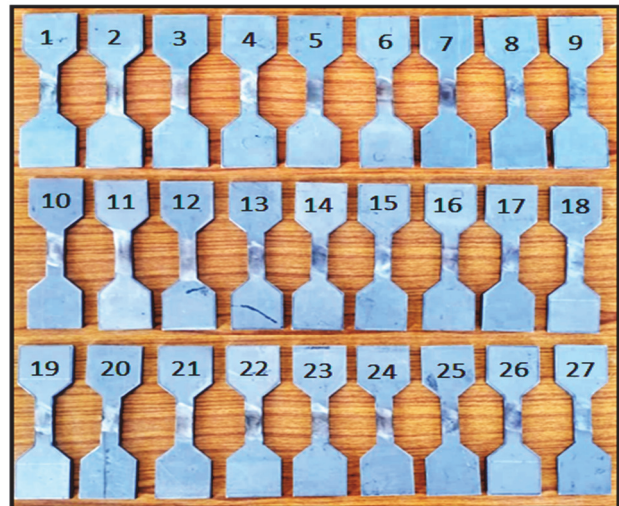


Figure 3 AISI410 TIG welded Tensile Specimen



Figure 4 UTM machine



Figure 5 Brinell hardness machine

Table 3 TIG welding input parameters and corresponding outputs responses

Iteration	Welding Current	Electrode Diameter	Wire Feed Rate	Gas Flow Rate	Tensile Strength	Hardness Test
Unit	Amps	mm	IPM	l/min	N/mm ²	(BHN)
1	240	2	250	20	1002	512
2	200	1.5	300	15	964	312
3	220	2.5	350	20	762	450
4	200	2	250	15	902	385
5	240	2	300	15	1090	510
6	240	1.5	300	20	1202	499
7	220	2	300	20	990	453
8	200	2	300	25	1168	501
9	200	2	300	15	936	450
10	220	1.5	300	15	950	400
11	240	2	350	20	1084	501
12	220	2	350	20	978	378
13	200	2	250	20	902	399
14	220	2	250	25	853	401
15	200	1.5	250	20	899	450
16	240	2	300	20	1004	503
17	220	1.5	350	20	901	435
18	200	2.5	300	20	978	380
19	240	2	300	25	1024	502
20	220	2	350	25	912	401
21	200	2	350	15	914	402
22	240	2.5	300	20	1084	500
23	220	2.5	300	25	914	403
24	200	1.5	300	25	976	378
25	240	2	300	20	1006	502
26	220	2.5	250	20	922	388
27	240	2.5	300	20	1032	510

The selected ranges of different TIG welding parameters like welding current, electrode diameter, wire feed rate, gas flow rate and selected output responses of tensile strength and hardness of the specimen values are shown in Tab. 3. From this table, it is observed that the maximum tensile values are achieved in maximum current of 240 Amp and highest values of 2 mm electrode diameter. The parameter of wire feed rate is not affecting the mechanical properties of tensile strength and the hardness of welded specimen. A better output response is achieved at the highest flow rate of 20 liter/min.

4 RESULTS AND DISCUSSION

4.1 Evaluation of TS and BHN

Based on the experimentation, for the required input parameters, the tensile strength and hardness were obtained randomly for the specifically dominated machining conditions. It is perceived that the higher tensile strength and hardness of fewer observations were obtained well. Especially, the input parameters of 240 A welding current using 2 mm diameter electrode for the wire feed rate of 300 IPM have given tremendous output values of tensile strength and hardness in the ranges starting from 1000 N/mm² up to maximum of 1202 N/mm². Likewise the BHN values also attained well between 500 BHN to 512 BHN respectively.

The Various TIG welding parameters are analyzed on austenitic stainless steels like AISI201, AISI 205, AISI 301, AISI 304L, AISI 316L. But martensitic stainless steel SS410 has not been analyzed with TIG welding parameters. The main novelty of this research work is that proper SEM images were analysed and inferences were included in each experiment. It is clear that the TIG welding parameters are the best values for achieving the best mechanical properties. In this research work, the martensitic stainless steel SS410 material is selected from literature survey. The standard TIG welding parameters are selected and the best optimization techniques implemented. The standard tensile specimen is prepared

and welded as per the optimization experimental runs. The tensile test is carried out in all the welded specimens and also SEM images are taken for all work pieces. From the SEM images, the Inferences are found and it is explained in details of all work pieces.

Hardness is measured at three different positions on welded zone using Brinell hardness machine and average values of BHN are selected in all specimens. The tests were carried out over the 27 sample specimens at three various spots of the welded area.

4.2 Optimization Procedure

The selected input parameters and their output responses are calculated with the various significant levels, and the best input TIG welding parameters are identified by using Design expert software. The tensile strength is analysed with partial sum of square Type III used forth is investigation. The Analysis of variance for various input and output responses is shown in Tab. 4. The F -value of 3.32 suggests that the data are significant. There is just a 1.64% chance that a "Model F -Value" could occur due to noise. Values of "Prob > F " less than 0.0500 and also A , A^2 indicators are significant.

The "Lack of Fit F -value" of 2765.36 implies that the Lack of Fit is significant. There is just a 1.50% chance that a "Lack of Fit F -value" this large could arise due to noise as shown in Tab. 5 and the final equation of actual factors for tensile test is given below.

$$\begin{aligned} \text{Tensile Strength} = & 7242.26393 - 84.53398 \cdot A + \\ & +197.49323 \cdot B + 16.76631 \cdot C + 5.44849 \cdot D + \\ & +0.19699 \cdot A^2 - 59.77615 \cdot B^2 - 0.027547 \cdot C^2 - \\ & -0.082633 \cdot D^2 \end{aligned}$$

where:

A - welding current; B - electrode diameter; C - wire feed rate; D - gas flow rate.

Table 4 Analysis of variance table for tensile strength

Source	Sum of Squares	DOF	Mean Square	F -value	p -value	Inferences
Model	138794.3	8	17349.2	3.32	0.016	Significant
A - Welding Current	26854.7	1	26854.7	5.14	0.035	predominantly influencing
B - Electrode Diameter	4874.7	1	4874.7	0.93	0.346	
C - Wire Feed Rate	1555.6	1	1555.6	0.29	0.592	
D - Gas Flow Rate	1277.0	1	1277.0	0.24	0.627	
A^2	26200.0	1	26200.0	5.01	0.038	
B^2	1170.1	1	1170.1	0.22	0.641	
C^2	21753.6	1	21753.6	4.16	0.056	
D^2	22.95	1	22.9	0.004	0.947	
Residual	94024.3	18	5223.5			
Lack of Fit	94022.3	17	5530.7	2765.3	0.015	
Pure Error	2	1	2			
Cor Total	232818.6	26				

Table 5 Lack of fit for tensile strength

Std. Dev.	Mean	C.V. %	PRESS	R -Squared	Adj R -Squared	Pred R -Squared	Adeq Precision
72.2	975.8	7.4	197138.3	0.597	0.417	0.154	5.915

The Hardness of the welded specimen is analysed and partial sum of square Type III is used for this investigation. The Analysis of variance for various input and output responses is shown in Tab. 6. The Model F -value of 4.54

implies that the model is significant. There is only a 0.37% chance that a "Model F -Value" could occur due to noise. Values of "Prob > F " less than 0.0500 indicate model terms

are significant. In this case A , A^2 are significant model terms.

The "Lack of Fit F-value" of 3280.23 implies that the Lack of Fit is significant. There is only a 1.37% chance that a "Lack of Fit F-value" could occur due to noise. It is mentioned in Tab. 7 and the final equation of actual factors for Brinell Hardness is:

$$\text{Brinell Hardness} = 4420.89011 - 42.70697 \cdot A + 257.67522 \cdot B + 1.21425 \cdot C - 1.60407 \cdot D + 0.10237 \cdot A^2 - 62.01304 \cdot B^2 - 1.96702e^{-003} \cdot C^2 + 0.048809 \cdot D$$

where: A - welding current; B - electrode diameter; C - wire feed rate; D - gas flow rate.

Table 6 Analysis of variance table for brinell hardness number

Source	Sum of Squares	DOF	Mean Square	F-value	p-value	Inferences
Model	56289.3	8	7036.1	4.55	0.0037	significant
A - Welding Current	31990.5	1	31990.5	20.6	0.0003	predominantly influencing
B - Electrode Diameter	260.7	1	260.7	0.169	0.6865	
C - Wire Feed Rate	31.7	1	31.757	0.0205	0.8877	
D - Gas Flow Rate	33.73	1	33.8	0.0218	0.8843	
A^2	7075.9	1	7075.9	4.57	0.0466	
B^2	1259.3	1	1259.3	0.813	0.3791	
C^2	110.92	1	110.9	0.071	0.7921	
D^2	8.008	1	8.0077	0.005	0.9435	
Residual	27882.5	18	1549.02			
Lack of Fit	27881.9	17	1640.1	3280.2	0.0137	
Pure Error	0.5	1	0.5			
Cor Total	84171.8	26				

Table 7 Lack of fit for hardness

Std. Dev.	Mean	C.V. %	PRESS	R-Squared	Adj R-Squared	Pred R-Squared	Adeq Precision
39.4	441	8.93	61054.9	0.67	0.5216	0.275	5.430

4.3 Three Dimensional Plots of Tensile Strength

From Fig. 6, it is observed that there is a gradual increase in tensile strength with increasing welding current. There is no drastic change in tensile strength with either increase or decrease in electrode diameter.

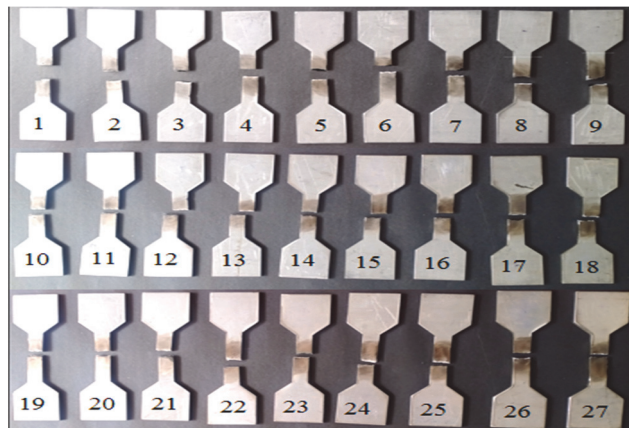


Figure 6 Tensile strength tested specimen samples

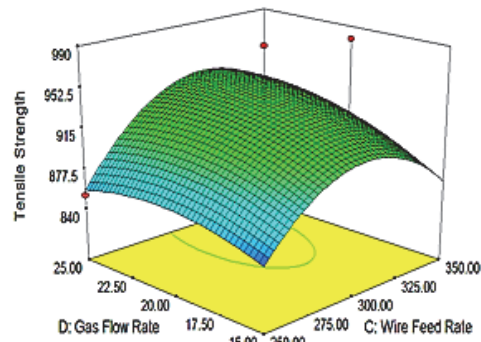


Figure 8 3D plot for tensile strength versus gas flow rate and wire feed rate

Fig. 7 clearly indicates that by the increase in wire feed rate the tensile strength increases gradually till a saturation point and then suddenly decreases. As far as gas flow rate is concerned, there is meagre rise in tensile strength with rising gas flow rate. Fig. 8 obtained from Predicted values for output responses of tensile strength, calculated using regression equation indicates good agreement with experimental values.

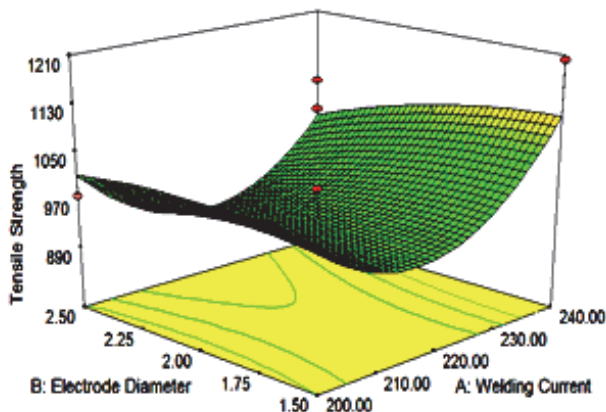


Figure 7 3D plot for tensile strength versus electrode diameter and welding current

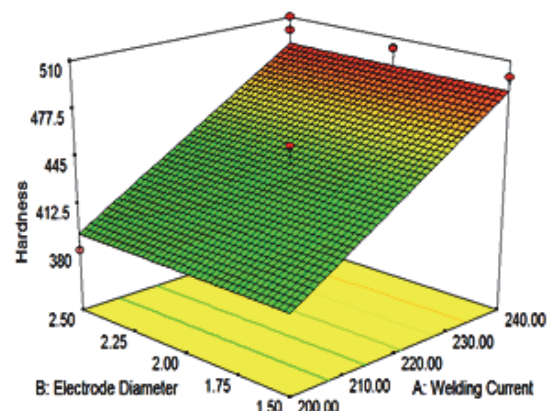


Figure 9 3D plot for brinell hardness number versus electrode diameter and welding current

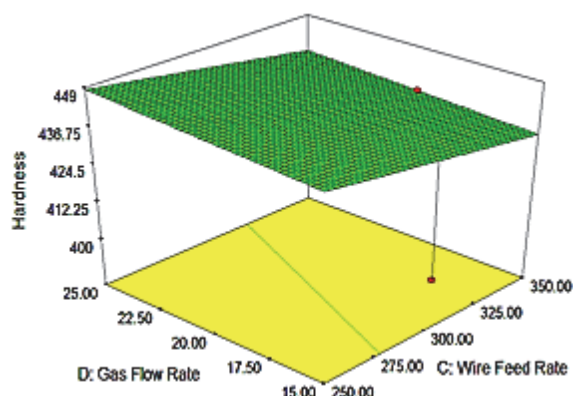


Figure 10 3D plot brinell hardness versus gas flow rate and wire feed rate

Welding current and electrode diameter vs. hardness. With increasing welding current, there is a steep increase in Brinell hardness values, as shown in the 3D plot. When the electrode diameter is increased, the Brinell hardness remains nearly constant, with no significant variations. The graph depicting the relationship between Brinell hardness and gas flow rate and wire feed rate clearly demonstrates that no dominant effect exists.

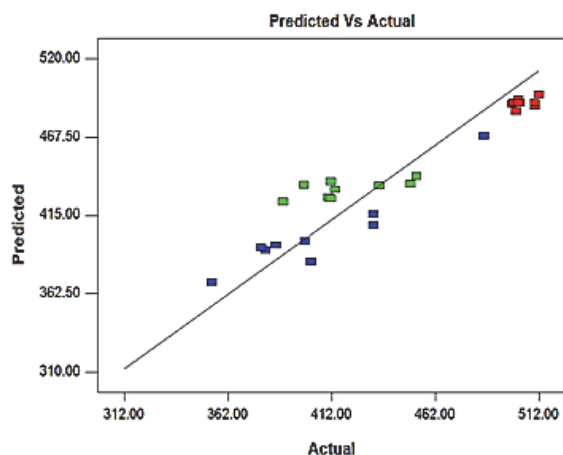


Figure 11 Predicted values for output responses of tensile strength

The Fig. 11 shows that all predicted results are nearer to the experimental values by more than 87%. The various TIG welding input parameters and output responses ranges are decided based on the literature review and welding kit specifications. The output values are decided as "Larger is Better" for both tensile strength and Brinell hardness number. The criteria for factors and responses are shown in Tab. 8. From Tab. 8, the maximum value of 1202 N/mm² is obtained for tensile strength and 512BHN is better for Brinell hardness number. The best TIG welding input parameters and output responses are calculated from Design Expert as shown in Tab. 8. The best possible of various factors and responses obtained from Design of Experiment (DOE) are given in Tab. 9.

Table 8 Criteria for factors and responses

Input and Output Responses	Goal	Lower Limit	Upper Limit
Welding Current	in range	200	240
Electrode Diameter	in range	1.5	2.5
Wire Feed Rate	in range	250	350
Gas Flow Rate	in range	15	25
Tensile Strength	Maximize	762	1202
Brinell Hardness	Maximize	312	512

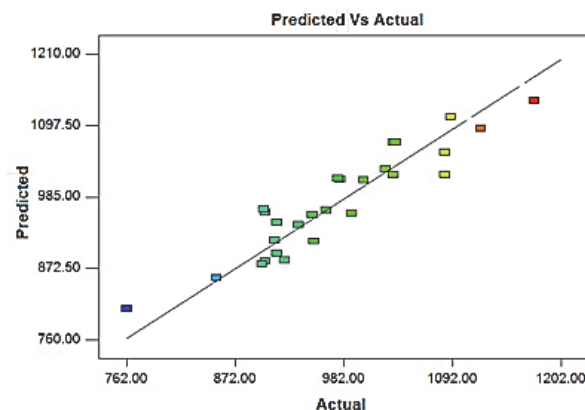


Figure 12 Predicted values for output responses of brinell hardness

Table 9 Best possible values for factors and responses

Welding Current	Electrode Diameter	Wire Feed Rate	Gas Flow Rate	UTS	BHN	Desirability	Decision
240	1.93	304.8	25	1095	511.89	0.89	Selected

5 SEM OBSERVATIONS AND ANALYSIS OF TIG WELDED SPECIMEN

The first ten iterations of various TIG welding parameters and corresponding SEM images are mentioned in Tab. 10. The SEM image is observed on cross section of the welded zone after tensile test. The SEM image taken from 7100 Hitachi, range of 20 μm is plotted with corresponding TIG Welding parameters. During tensile testing, a small cleavage will form in the breaking zone at the end of the tensile strength. The cleavage is clearly visible in the welded zone in iterations 6, 7, and 8, and the remaining parameters are formed with various defects such as dimples, microvoids, and various types of fractures.

The iteration from 11 to 20, the SEM image for corresponding TIG welding input parameters are shown in Tab. 11. The iteration number 11, 12 and 14 clearly identified the cleavage formation of the welded zone. The

remaining iterations are affected with the various types of Dimples.

The iterations from 21 to 27, the SEM image for corresponding TIG welding input parameters are shown in Tab. 12. The actual cleavage is presented in the 27th iteration number. The remaining iterations are affected with the various types of cracks and Dimples.

In Tabs. 10, 11 and 12 it is observed that the various types of dimples, microvoids and fractures are not suitable for automobile parts. During tensile test, the cleavage formations only may appear on the welded zone. The actual cleavage is formed in several parameters and it is strongly recommended for the welding application.

Fig. 13 depicts the variations of hardness values and tensile strengths in vertical primary y axis for the corresponding influencing factor of welding current located in the vertical secondary y axis. The hardness values are randomly increased for the highlighted values of

machining conditions, which have been indicated with the yellow markers. More tensile strength was observed at the beginning of the sample numbers. The similar kind of

increase and decrease of peaks has been obtained for both tensile strength and hardness values.

Table 10 SEM analyses of TIG welded specimens

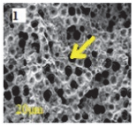
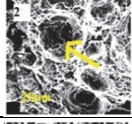
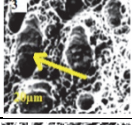
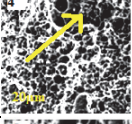
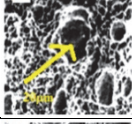
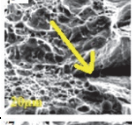
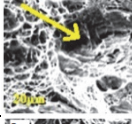
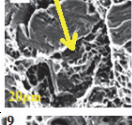
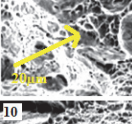
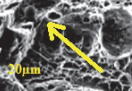
Iteration	Welding Current	Electrode Diameter	Wire Feed Rate	Gas Flow Rate	SEM Image	Inferences
Unit	Amps	mm	IPM	l/min	20 μm	
1	240	2	250	20		Microvoid coalescence found in several places
2	200	1.5	300	20		Large dimples are presented
3	220	2.5	350	20		Elongated dimples are presented
4	220	2	250	15		Small cleavage is presented
5	240	2	300	15		More number of medium dimples are presented
6	240	1.5	300	20		Normal cleavage is presented
7	220	2	300	20		Curved cleavage is presented
8	200	2	300	25		New type of transgranular cleavage is presented
9	200	2	300	15		Box fatigue portion is presented
10	220	1.5	300	15		Deep dimples are presented

Table 11 SEM analyses of TIG welded specimens

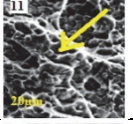
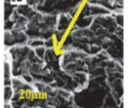
Iteration	Welding Current	Electrode Diameter	Wire Feed Rate	Gas Flow Rate	SEM Image	Inferences
Unit	Amps	mm	IPM	l/min	20 μm	
11	240	2	350	20		Small transgranular cleavage is presented
12	200	2	350	20		Several transgranular cleavages are presented

Table 11 SEM analyses of TIG welded specimens (continuation)

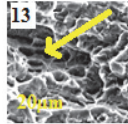
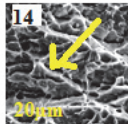
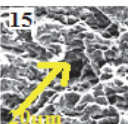
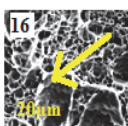
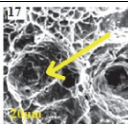
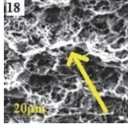
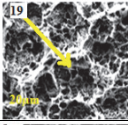
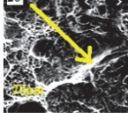
Iteration	Welding Current	Electrode Diameter	Wire Feed Rate	Gas Flow Rate	SEM Image	Inferences
Unit	Amps	mm	IPM	l/min	20 μ m	
13	200	2	250	20		Microvoid is presented
14	220	2	250	25		Dual transgranular cleavages are presented
15	220	1.5	250	20		Dimple is presented in the mid places
16	220	2	300	20		Cave dimples are presented
17	220	1.5	350	20		Small lunar dimple is presented
18	200	2.5	300	20		Dimpled Rupture fracture is presented
19	240	2	300	25		Equiaxed dimples are presented
20	220	2	350	25		Actual cleavage is presented

Table 12 SEM analyses of TIG welded specimens

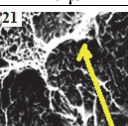
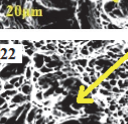
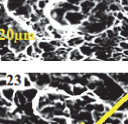
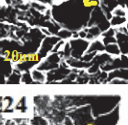
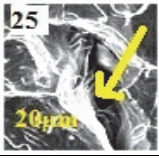
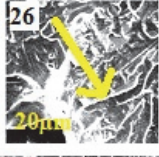
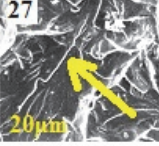
Iteration	Welding Current	Electrode Diameter	Wire Feed Rate	Gas Flow Rate	SEM Image	Description
Unit	Amps	mm	IPM	l/min	20 μ m	
21	220	2	350	15		Deep cleavage is presented
22	220	2.5	300	15		Microvoid is presented
23	220	2.5	300	25		Small lunar dimple is presented
24	220	1.5	300	25		Cave dimples are presented

Table 12 SEM analyses of TIG welded specimens (continuation)

Iteration	Welding Current	Electrode Diameter	Wire Feed Rate	Gas Flow Rate	SEM Image	Description
Unit	Amps	mm	IPM	l/min	20 μm	
25	220	2	300	20		Crack cleavage is presented
26	220	2.5	250	20		Crack cleavage is presented
27	240	2.5	300	20		Actual cleavage is presented

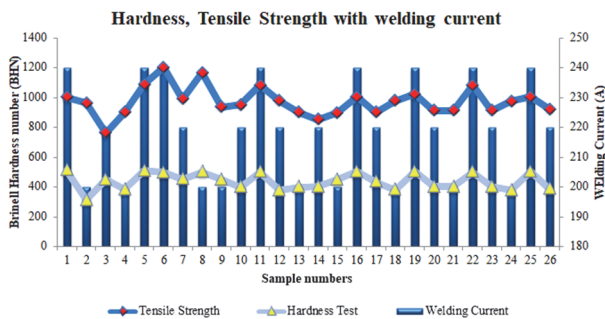


Figure 13 Correlation of hardness, tensile strength for the welding current

The exact correlations have been maintained between the tensile strength and hardness values, as shown in Fig. 14. Eventhough the wire feed rate is not significant, it can coincide with the tensile strength and hardness values.

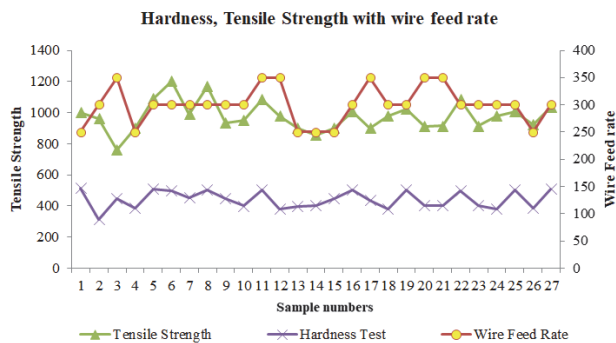


Figure 14 Correlation of hardness, tensile strength for the wire feed rate

6 CONCLUSION

Various necessary input parameters were used for testing in TIG welding, and mechanical properties and SEM analyses were discussed in this investigation. For this experiment, welding input process parameters such as welding current, electrode diameter, gas flow rate, and wire feed rate were used. Tensile strength and specimen hardness (BHN) were considered as the output responses. The following conclusions have been drawn from the experimental data:

- The input factor involved in TIG welding, welding current of 240 A with a *p*-value of 0.0359 is found to be the most significantly influencing parameter on tensile strength. The secondary level of less influence was made by the electrode size of 2 mm in diameter. The effect of other parameters namely electrode diameter, gas flow rate and wire feed rate are not significant when compared to welding current.
- The input factor of welding current 240 A has a predominant effect on Brinell Hardness with *p*-value of 0.0003. Electrode diameter 2 mm has influenced mildly over BHN and TS. The gas flow rate and wire feed rate do not have any major effect on hardness at welded zone.
- From SEM characterization, the clear cleavage formations were formed on seven combinations of TIG welding parameters. Other combinations of welding parameters are affected with various fracture defects like dimples, caves, cracks, microvoid and rupture fractures.
- The best possible values of the input parameters, like 240 A of welding current, 2 mm of electrode diameter, 300 IPM of wire feed rate and a gas flow rate with 25 liter/min have yielded the best results.

Acknowledgements

The authors would like to thank their Research Supervisors, Technicians for their esteemed guidance and technical support throughout the research. The author would also wish to acknowledge the co-authors for supporting this research project.

7 REFERENCES

[1] Sharma, N., Abdullaha, W. S., Garg, M., Gupta, R. D., Khanna, R., & Sharma, R. C. (2020). Optimization of TIG Welding Parameters for the 202 Stainless Steel Using NSGA-II. *Journal of Engineering Research*, 8(4), 206-221. <https://doi.org/10.36909/jer.v8i4.7071>

[2] Rizvi, S. A. & Ali, W. (2018). Optimization of Welding Parameters and Microstructure and Fracture Mode Characterization of GMA Welding by Using Taguchi

- Method on SS304H Austenitic Steel. *Mechanics and Mechanical Engineering*, 22(4), 1121-1131. <https://doi.org/10.2478/mme-2018-0088>
- [3] Loureiro, A. & Rodrigues, A. (2008). A-TIG welding of a stainless steel. *Materials Science Forum*, 587-588, 370-374. <https://doi.org/10.4028/www.scientific.net/MSF.587-588.370>
- [4] Ahmadi, E. & Ebrahimi, A. R. (2015). Welding of 316L Austenitic Stainless Steel with Activated Tungsten Inert Gas Process ASM International. *Journal of Materials Engineering and Performance*, 24, 1065-1071. <https://doi.org/10.1007/s11665-014-1336-6>
- [5] Vasudevan, M. (2017). Effect of A-TIG Welding Process on the Weld Attributes of Type 304LN and 316LN Stainless Steels. *Journal of Materials Engineering and Performance*, 26, 1325-1336. <https://doi.org/10.1007/s11665-017-2517-x>
- [6] Garg, H., Karanshegal, L. R., & Kajal, G. (2019). A Systematic Review: Effect of TIG and A-TIG Welding on Austenitic Stainless Steel. *Advanced Industrial and Production Engineering*, 2, 375-385. https://doi.org/10.1007/978-981-13-6412-9_36
- [7] Ghosh, N., Pal, P. K., & Nandi, G. (2016). Parametric optimization of MIG welding on 316L austenitic stainless steel by Taguchi method. *Archives of Materials Science and Engineering*, 79(1), 27-36. <https://doi.org/10.5604/18972764.1227660>
- [8] Mahesh, G., Kumar, K. M. M., Bharathi Raja, S., Baskar, N., & Ganesan, M. (2017). Experimental Investigation and Optimization of Hardness in Sand Casting Process by Using the Design of Experiments Approach. *Applied Mathematics and Information Science*, 11(3), 931-938. <https://doi.org/10.18576/amis/110334>
- [9] Maheshwaran, S. & Senthilkumar, T. (2017). Experimental Investigation on Mechanical Property of MIG Welding Process. *International Journal of Engineering Research & Technology*, 5(13), 1-4.
- [10] Somani, C. A. & Lalwani, D. I. (2019). Experimental Investigation of TIG-MIG Hybrid Welding Process on Austenitic Stainless Steel. *Materials Today Proceeding*, 18(4), 4826-4834. <https://doi.org/10.1016/j.matpr.2019.07.472>
- [11] Singhmar, M. & Verma, N. (2015). Experimental Study for Welding Aspects of Austenitic Stainless Steel (AISI 304) on Tensile Strength by Taguchi Technique. *International journal of Mechanical Engineering and Robotics Research*, 4(1), 493-503.
- [12] Feng, Y. Q., Luo, Z., Liu, Z. M., Li, Y., Luo, Y.C., & Huang, Y. X. (2015). Keyhole gas tungsten arc welding of AISI 316L stainless steel. *Materials and Design*, 85, 24-31. <https://doi.org/10.1016/j.matdes.2015.07.011>
- [13] Bharwal, S. & Vyas, C. (2014). Weldability Issue of AISI 202 SS (Stainless Steel) Grade with GTAW Process Compared to AISI 304 SS Grade. *International Journal of Advanced Mechanical Engineering*, 4(6), 695-700.
- [14] Rekha, Y. & Kajal, G. (2018). Process Parameter Selection for Optimizing the Mechanical Properties of Stainless Steel (SS 202 & SS 316) in the Gas Tungsten Arc Welding. *International Journal for Research in Applied Science & Engineering Technology*, 6(4), 2684-2695. <https://doi.org/10.22214/ijrasnet.2018.4449>
- [15] Suresh Kumar, L., Verma, S. M., Prasad, P. R., Kirankumar, P., & Siva Shanker, T. (2011). Experimental Investigation for Welding Aspects of AISI 304 & 316 by Taguchi Technique for the Process of TIG & MIG Welding. *International Journal of Engineering Trends and Technology*, 2(2), 28-33.
- [16] Ghiasvand, A., Kazemi, M., & Jalilian M. (2020). Effects of tool offset, pin offset, and alloys position on maximum temperature in dissimilar FSW of AA6061 and AA5086. *International Journal of Mechanical and Materials Engineering*, 15, 6. <https://doi.org/10.1186/s40712-020-00118-y>
- [17] Kazemi, M., & Ghiasvand, A. (2021). Effect of cone angle of cylindrical pin in the SFSW and DFSW on mechanical properties of AA6061-T6 alloy. *International Journal of Mechanical and Materials Engineering*, 16, 8. <https://doi.org/10.1186/s40712-021-00131-9>
- [18] Ghiasvand, A., Kazemi, M., & Mahdipour Jalilian, M. (2020). Numerical investigation and prediction of grain Size in different friction stir welding areas of AA6061 Aluminum alloy. *Amirkabir (Journal of Science and Technology)*.
- [19] Bejaxhin, A. B. H., Balamurugan, G. M., Sivagami, S. M., Ramkumar, K., Vijayan, V., & Rajkumar, S. (2021). Tribological Behavior and Analysis on Surface Roughness of CNC Milled Dual Heat Treated Al6061 Composites. *Advances in Materials Science and Engineering*, 3844194, 14. <https://doi.org/10.1155/2021/3844194>

Contact information:

Dr. G. MAHESH, Associate Professor
Saranathan College of Engineering,
Panjappur, Trichy
E-mail: mahesh-mech@saranathan.ac.in

Dr. D. VALAVAN, Professor
Saranathan College of Engineering,
Panjappur, Trichy
E-mail: valavand@gmail.com

Dr. M. BASKAR, Professor
Saranathan College of Engineering,
Panjappur, Trichy
E-mail: baskar-mech@saranathan.ac.in

Dr. A. BOVAS HERBERT BEJAXHIN
(Corresponding author)
Associate Professor - Mechanical Engineering,
Saveetha School of Engineering,
SIMATS, Thandalam, Chennai
E-mail: herbert.mech2007@gmail.com